


Product Selection and Supply Chain Optimization for Fast Pyrolysis and Biorefinery System

Yanan Zhang[†] and Mark M. Wright*

Department of Mechanical Engineering, Iowa State University, Ames, Iowa 50011, United States

 Supporting Information

ABSTRACT: This study determines the optimal plant sizes, locations, and product distributions for an integrated fast pyrolysis biorefinery supply chain using a mixed-integer nonlinear programming (MINLP) model. Hydrogen, liquid fuels, commodity chemicals, and lignin are considered as the potential biorefinery products. The proposed approach is illustrated through a case study of Minnesota, where forest residue is selected as the biomass feedstock. The decisions about biomass supply (roadside chipped forest residue and raw forest residue), facility selection, and product distribution are explored in this case study. The total converted bio-oil is 1.1 million metric tons per year and the total cost is \$330 million for the base case. Impacts of marketing prices on product selections are investigated. Compared to upgrading of phase separated bio-oil, whole bio-oil upgrading is preferable in terms of economics. Hydrogen and liquid fuel prices have greater influence on the annualized profit than the commodity chemical price.

1. INTRODUCTION

As required by the Energy Independence and Security Act of 2005,¹ the U.S. Environmental Protection Agency (EPA) regulates the supply of renewable transportation fuels consumed in the U.S. through the Renewable Fuel Standard (RFS2) program. Refiners, renewable fuel producers, and other stakeholders are mandated to meet annual biofuel volumes and environmental requirements in order to comply with the RFS2. Despite drastic growth in the production of renewable ethanol from corn grain, several techno-economic challenges and financing constraints have limited the supply of advanced biofuels.²

A potential pathway to the production of advanced biofuels is the conversion of forest residues into gasoline and diesel via fast pyrolysis and upgrading.³ Fast pyrolysis is a rapid thermal decomposition of organic compounds in the absence of oxygen to produce liquids, char, and gas. Fast pyrolysis for biofuel production is currently of particular interest as the liquid product can be readily stored and transported, which is beneficial when biomass resources are remote from demand locations.^{4,5} Furthermore, fast pyrolysis and its primary product, bio-oil, could offer versatile processing routes to a wide range of products and contribute to the development of the biorefinery concept.⁴ A biorefinery based on fast pyrolysis could produce hydrogen, chemicals, heat, power, and transportation fuels.^{6–11}

Driven by the growing interest in fast pyrolysis technology, considerable research has been conducted on the economic, environmental, logistic, and social issues related to energy and fuels production from biomass fast pyrolysis and upgrading. It has been shown that converting biomass to transportation fuels via fast pyrolysis is economically feasible.^{12–15} In addition, the greenhouse gas (GHG) emissions and net energy input could be largely reduced if transportation fuels are produced via fast pyrolysis and upgrading compared to the conventional petroleum pathways.^{16–18}

In addition to the study of economics, environmental, and social issues, numerous studies have been devoted to optimal design and operation planning of the products derived from the fast pyrolysis pathway.^{19–22} Tong et al.²³ has developed the optimal design and strategic planning of the integrated biofuel and petroleum supply chain system with fast pyrolysis technology in the presence of pricing and quantity uncertainties. Gebreslassie et al.²² developed a biofuels production analysis by presenting a bicriterion, multiperiod, stochastic mixed-integer linear programming model to address the optimal design of hydrocarbon biorefinery supply chains under supply and demand uncertainties. Two pathways were considered for this model, which are gasification followed by FT synthesis and fast pyrolysis followed by hydroprocessing. Kim et al.¹⁹ formulated a general MILP model to design and analyze optimal distributed and centralized processing network systems that process biomass into bio-oil and then to biodiesel and gasoline. Kim et al.²⁴ also developed an optimization-based assessment framework to identify the optimal biomass-to-fuel conversion strategy based on an analyzed biomass utilization superstructure.

Recently, geographic information systems (GIS) were incorporated into the biofuels supply chain design to compute more accurately the expected regional biomass availability along with the transportation distances and related costs for the supply chain design. Panichelli and Edgard²⁵ presented a GIS-based decision support system for selecting least-cost bioenergy locations when there is a significant variability in biomass farm gate price and when more than one bioenergy plant with a fixed capacity has to be placed in the region. Zhang et al.²⁶ developed a two-stage methodology to identify the best location for

Received: September 8, 2014

Revised: November 15, 2014

Accepted: November 25, 2014

Published: November 25, 2014

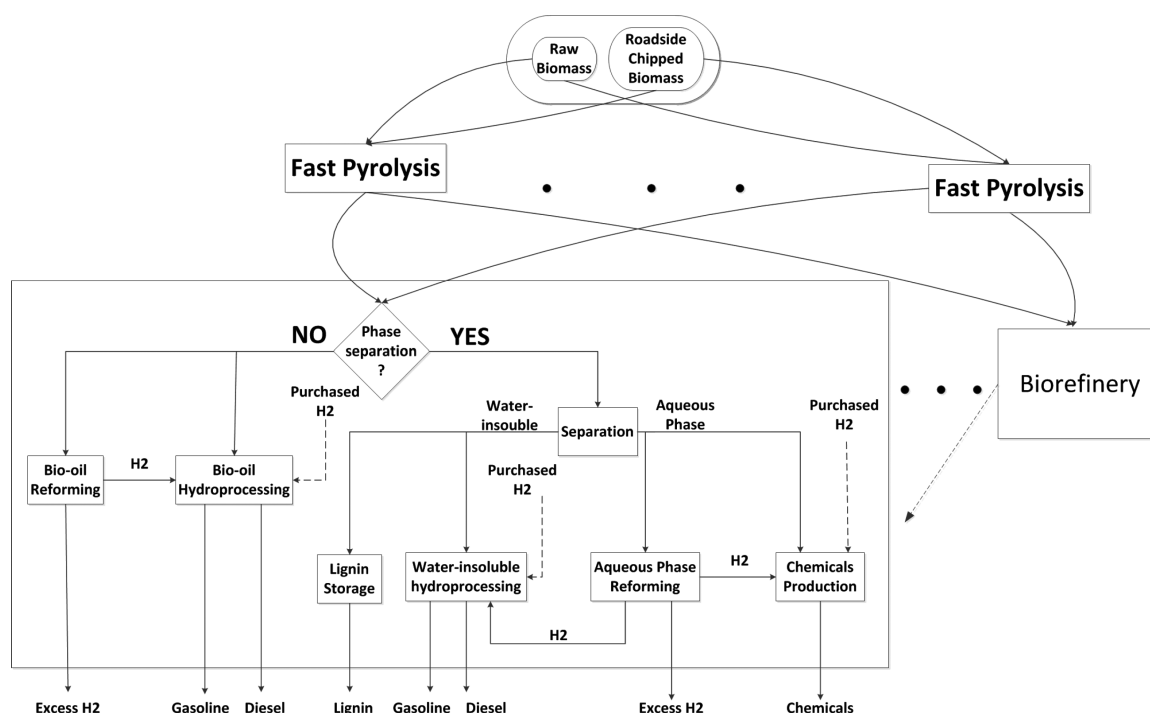


Figure 1. Supply chain material and product selection optimization diagram.

biofuel production based on multiple attributes. Stage I uses a GIS approach to identify feasible biofuel facility locations and stage II selected the preferred location using a total transportation cost model. Lin et al.²⁷ developed a GIS-enabled biomass supply chain optimization model (BioScope) to minimize annual biomass–ethanol production costs by selecting the optimal numbers, locations, and capacities of farms, centralized storage and preprocessing (CSP) sites, and biorefineries as well as identifying the optimal biomass flow pattern from farms to biorefineries. Zhang et al.²⁸ presented a GIS-based multiobjective optimization model to analyze the trade-off between the economic and environmental considerations for commodity chemicals production.

Some researchers focus on the strategic elements of biofuels production including feedstock, technologies, and production route selections, and product portfolio optimization. Sammons Jr.²⁹ has developed a mathematical optimization based framework to enable the inclusion of profitability measures and other techno-economic metrics to identify the optimal set of products and the best route for production for the biorefinery. Murillo-Alvarado³⁰ developed a generalized disjunctive programming model that accounts for the simultaneous selection of products, feedstocks, and processing steps. The optimal solution can involve multiproduct and multifeedstock biorefineries. Mansoornejad³¹ has presented one methodology that links the product/process portfolio design and supply chain design to build a design decision making framework. Through this methodology, the market volatility effects are investigated. Chen et al.³² developed a MILP model to investigate a static energy polygeneration system coproducing power, liquid fuels, and chemicals from coal and biomass as feedstock. Optimal product portfolios are obtained under different product price scenarios. Chen et al.³³ also proposed a two-stage programming formulation to optimize simultaneously the design decision variables and the operational decision variables for flexible polygeneration systems using coal and

biomass to coproduce power, liquid fuels, and chemicals. In that study, they also discussed the optimal product portfolios, equipment capacity usages, and CO₂ emissions of flexible polygeneration systems under different market conditions.

Although many studies focus on the supply chain design for biofuels production from fast pyrolysis, most of the papers concentrate on technology selection for liquid fuels. Very few papers incorporate other biorefinery products such as hydrogen and commodity chemicals from a fast pyrolysis system. In this paper, a supply chain network coupling process portfolio design is developed using mixed-integer nonlinear programming (MINLP) modeling with GIS analysis to optimize the product selection and locations and capacities of chemical production from fast pyrolysis and biorefinery. A case study for the State of Minnesota is presented to illustrate the integrated supply chain network design model with the biomass feedstock of forest residue.

2. METHODOLOGY

2.1. Supply Chain Model Description. The purpose of this study is to determine the optimal plant sizes, locations, biomass inputs, and product distributions for an integrated fast pyrolysis biorefinery within a supply chain design framework. There are six subscripts related to candidate harvest and facility locations, possible facility capacity levels, chemical species, and segments for capital linearization. Decision variables include binary decisions related to the facility deployment at a given location and the implementation of specific unit operations within the facility. Continuous decision variables include material flows for facility inputs, intermediates, and final products; split fractions for separations processes; and capital cost.

Figure 1 illustrates the supply chain network schematic for product optimization via woody biomass fast pyrolysis and upgrading. First, the woody biomass is collected from harvest sites. Second, fast pyrolysis facilities at optimal locations

convert the biomass into bio-oil, biochar and noncondensable gases that are consumed within the process. Finally, the bio-oil is transported to biorefinery facilities where it is upgraded into a suite of chemicals and/or fuels. The model considers two types of woody biomass: raw forest residue and the residue chipped with a road-side chipping method. Both types of biomass can be converted into bio-oil, which is the primary intermediate material in the supply chain.

Bio-oil can be separated into aqueous and water-insoluble phases. Upgrading these phases can yield a variety of chemicals and/or fuels. In this paper, we considered scenarios with and without phase separation of the bio-oil. First, the model decides whether to phase separate the bio-oil. In the scenario without bio-oil phase separation, a portion of the bio-oil could be either hydroprocessed to gasoline and diesel fuel, or reformed to hydrogen. The model determines the split ratio of bio-oil for hydrogen production or gasoline and diesel fuel. Hydro-processing bio-oil requires hydrogen input, which can be generated by reforming bio-oil or by purchasing from an external source.³⁴ The model determines the optimal amount of hydrogen generation or purchase for each scenario. The model could also consider generating excess hydrogen as a coproduct with gasoline and diesel fuel. In the scenario of bio-oil phase separation, the bio-oil is divided into water-soluble phase and aqueous phase. The aqueous phase contains light oxygenated compounds and could be reformed to either hydrogen or commodity chemicals. The model determines the split ratio of aqueous phase bio-oil for hydrogen or chemical synthesis. On the other hand, the water-insoluble phase could be treated as lignin or hydroprocessed to gasoline and diesel fuels depending on the optimal split ratio. As in the previous case, requisite hydrogen for chemical synthesis or water-insoluble phase hydroprocessing could be generated from aqueous phase reforming or purchased from a merchant source depending on the optimal decision determined by the model. Excess hydrogen could also be considered in this scenario. In this model, the hydrogen delivery and infrastructure are not taken into account.

2.2. Model Formulation. **2.2.1. Biomass Supply Constraints.** This section describes the mass balance of biomass flows and facility capacity constraints. The total biomass collected F_i should not exceed the available biomass A_i for collection in harvesting location i . In eq 1, α is the sustainability factor, which limits the allowed collection to a percentage of the available biomass.

$$F_i \leq \alpha A_i, \quad \forall i \quad (1)$$

The total collected biomass F_i can be categorized into two types: raw biomass and roadside chipped biomass. They both can be transported to the fast pyrolysis facility location j . In eqs 2 and 3, x_{ij} and y_{ij} are the amount of transported raw biomass and roadside chipped biomass from harvest location i to fast pyrolysis location j . Here ε is the loss factor for the biomass transportation process and B_j is the total received biomass (raw biomass and roadside chipped biomass) in fast pyrolysis facility location j .

$$\sum_{j=1}^J (x_{ij} + y_{ij}) = F_i(1 - \varepsilon), \quad \forall i \quad (2)$$

$$\sum_{i=1}^I (x_{ij} + y_{ij}) = B_j, \quad \forall j \quad (3)$$

2.2.2. Fast Pyrolysis Facility Constraints. The fast pyrolysis facility constraints are shown in eqs 4–8. Biomass input to the facility at location j should not exceed the total facility capacity at that location $\text{Cap}_j^{\text{pyro}}$.

$$B_j \leq \sum_{l=1}^L \text{Cap}_l^{\text{pyro}} r_{lj}, \quad \forall j \quad (4)$$

For each candidate location j , there is at most one facility with capacity level l .

$$\sum_{l=1}^L r_{lj} \leq 1, \quad \forall j \quad (5)$$

The total number of fast pyrolysis facilities at location j with capacity level l should not exceed the maximum number Num^{pyro} .

$$\sum_{l=1}^L \sum_{j=1}^J r_{lj} \leq \text{Num}^{\text{pyro}}, \quad \forall j \quad (6)$$

In eq 7, biochar is generated as a factor β^{char} of the received biomass. For eqs 8 and 9, the received biomass B_j is processed with a bio-oil yield β^{oil} of H_j at fast pyrolysis facility location j and then bio-oil H_j is transported by truck to the biorefinery location k .

$$B_j \beta^{\text{char}} = p_j^{\text{char}}, \quad \forall j \quad (7)$$

$$B_j \beta^{\text{oil}} = H_j, \quad \forall j \quad (8)$$

$$\sum_{k=1}^K z_{jk} = H_j, \quad \forall j \quad (9)$$

2.2.3. Biorefinery Constraints. The total bio-oil received in biorefinery facility location k is presented as T_k (eq 10). In the biorefinery facility location k , the bio-oil T_k could be converted to different products. Here ρ_k is a binary variable that determines whether the bio-oil should be separated into water-soluble and water-insoluble phases in location k . The aqueous phase bio-oil yield and water-insoluble phase bio-oil yield is presented in eqs 11 and 12. Here θ^{aqu} and θ^{insol} are the aqueous phase and water-insoluble phase weight percentages of the whole bio-oil. Part of the aqueous phase bio-oil is used to produce hydrogen via a reforming process, and the quantity of hydrogen generated from aqueous phase reforming ($p_k^{\text{hydro},1}$) is calculated in eq 13. Here $f_k^{\text{aqu},1}$ is the split ratio of aqueous phase bio-oil that is used to produce hydrogen via the reforming process and $\theta^{\text{hydro},1}$ is the hydrogen conversion rate based on the aqueous phase bio-oil. The remaining aqueous phase bio-oil is used to produce chemicals. Here in eq 14, θ_w^{chem} is the conversion rate for specific chemical w , and p_{kw}^{chem} is the production quantity of chemical w at location k . The required hydrogen for chemical synthesis is calculated in eq 15, where $\delta^{\text{hydro},1}$ means the required hydrogen factor based on the aqueous phase bio-oil, and $n_k^{\text{hydro},1}$ is the total required hydrogen amount for chemical synthesis. The total hydrogen input includes purchased hydrogen ($p_k^{\text{mechhydro},1}$) and the split hydrogen from aqueous phase bio-oil reforming ($p_k^{\text{hydro},1} s_k^{\text{aqu},1}$) (eq 16). Here $s_k^{\text{aqu},1}$ is the split ratio of hydrogen generated from aqueous phase bio-oil reforming for chemical synthesis.

Equations 17–22 describe the mass balance for the water-insoluble bio-oil phase. The water-insoluble phase could be

divided into two parts. One part could be upgraded to gasoline and diesel fuel, and the other part could be stored as a lignin coproduct. The production of lignin, gasoline, and diesel fuel are calculated in eqs 17–19. The required hydrogen for water-insoluble phase bio-oil hydroprocessing ($n_k^{\text{hydro},2}$) is calculated in eq 20, where $f_k^{\text{insol},2}$ is the split ratio of water-insoluble phase bio-oil that is used to produce gasoline and diesel fuel, and $\delta^{\text{hydro},2}$ is the required hydrogen factor based on the water-insoluble bio-oil phase. The total required hydrogen ($n_k^{\text{hydro},2}$) includes purchased hydrogen ($p_k^{\text{mchanthydro},2}$) and the split hydrogen from aqueous phase bio-oil reforming ($p_k^{\text{hydro},1} s_k^{\text{aqu},2}$) (eq 21). Here $s_k^{\text{aqu},2}$ is the split ratio of hydrogen generated from aqueous phase bio-oil reforming for gasoline and diesel fuel production. The remaining hydrogen generated from aqueous phase bio-oil reforming is calculated in eq 22. Here $s_k^{\text{aqu},3}$ is the remaining hydrogen ratio based on aqueous phase bio-oil. Equations 23–25 are the constraints and mass balances for all of the split ratios.

$$\sum_{j=1}^J z_{jk} = T_k, \quad \forall k \quad (10)$$

$$T_k \rho_k \theta^{\text{aqu}} = p_k^{\text{aqu}}, \quad \forall k \quad (11)$$

$$T_k \rho_k \theta^{\text{insol}} = p_k^{\text{insol}}, \quad \forall k \quad (12)$$

$$p_k^{\text{aqu}} f_k^{\text{aqu},1} \theta^{\text{hydro},1} = p_k^{\text{hydro},1}, \quad \forall k \quad (13)$$

$$p_k^{\text{aqu}} f_k^{\text{aqu},2} \theta_w^{\text{chem}} = p_{kw}^{\text{chem}}, \quad \forall k \quad (14)$$

$$p_k^{\text{aqu}} f_k^{\text{aqu},2} \delta^{\text{hydro},1} = n_k^{\text{hydro},1}, \quad \forall k \quad (15)$$

$$p_k^{\text{mchanthydro},1} + p_k^{\text{hydro},1} s_k^{\text{aqu},1} = n_k^{\text{hydro},1}, \quad \forall k \quad (16)$$

$$p_k^{\text{insol}} f_k^{\text{insol},1} = p_k^{\text{lignin}}, \quad \forall k \quad (17)$$

$$p_k^{\text{insol}} f_k^{\text{insol},2} \theta^{\text{gaso},1} = p_k^{\text{gaso},1}, \quad \forall k \quad (18)$$

$$p_k^{\text{insol}} f_k^{\text{insol},2} \theta^{\text{diesel},1} = p_k^{\text{diesel},1}, \quad \forall k \quad (19)$$

$$p_k^{\text{insol}} f_k^{\text{insol},2} \delta^{\text{hydro},2} = n_k^{\text{hydro},2}, \quad \forall k \quad (20)$$

$$p_k^{\text{mchanthydro},2} + p_k^{\text{hydro},1} s_k^{\text{aqu},2} = n_k^{\text{hydro},2}, \quad \forall k \quad (21)$$

$$p_k^{\text{hydro},1} s_k^{\text{aqu},3} = p_k^{\text{excesshydro},1}, \quad \forall k \quad (22)$$

$$f_k^{\text{insol},1} + f_k^{\text{insol},2} = \rho_k, \quad \forall k \quad (23)$$

$$s_k^{\text{aqu},1} + s_k^{\text{aqu},2} + s_k^{\text{aqu},3} = \rho_k, \quad \forall k \quad (24)$$

$$f_k^{\text{aqu},1} + f_k^{\text{aqu},2} = \rho_k, \quad \forall k \quad (25)$$

Equations 26–35 show the constraints for the bio-oil upgrading without phase separation. Equation 26 presents the amount of bio-oil without phase separation. In eqs 27–29, the bio-oil without phase separation is divided into two parts, one is to produce hydrogen and the other part is to produce gasoline and diesel fuel. Equation 30 calculates the required hydrogen ($n_k^{\text{hydro},3}$) for the bio-oil hydroprocessing process. Equation 31 shows that the required hydrogen comes from the purchased hydrogen ($p_k^{\text{mchanthydro},3}$) and split hydrogen from bio-oil reforming ($p_k^{\text{hydro},2} s_k^{\text{oil},1}$). The remaining hydrogen generated

from bio-oil reforming is calculated in eq 32. Here $s_k^{\text{oil},2}$ is the remaining ratio of hydrogen. Equations 33 and 34 are the constraints of the split ratios $f_k^{\text{oil},1}$, $f_k^{\text{oil},2}$, $s_k^{\text{oil},1}$, and $s_k^{\text{oil},2}$.

$$T_k(1 - \rho_k) = p_k^{\text{oil}}, \quad \forall k \quad (26)$$

$$p_k^{\text{oil}} f_k^{\text{oil},1} \theta^{\text{hydro},2} = p_k^{\text{hydro},2}, \quad \forall k \quad (27)$$

$$p_k^{\text{oil}} f_k^{\text{oil},2} \theta^{\text{gaso},2} = p_k^{\text{gaso},2}, \quad \forall k \quad (28)$$

$$p_k^{\text{oil}} f_k^{\text{oil},2} \theta^{\text{diesel},2} = p_k^{\text{diesel},2}, \quad \forall k \quad (29)$$

$$p_k^{\text{oil}} f_k^{\text{oil},2} \delta^{\text{hydro},3} = n_k^{\text{hydro},3}, \quad \forall k \quad (30)$$

$$p_k^{\text{mchanthydro},3} + p_k^{\text{hydro},2} s_k^{\text{oil},1} = n_k^{\text{hydro},3}, \quad \forall k \quad (31)$$

$$p_k^{\text{hydro},2} s_k^{\text{oil},2} = p_k^{\text{excesshydro},2}, \quad \forall k \quad (32)$$

$$f_k^{\text{oil},1} + f_k^{\text{oil},2} = 1 - \rho_k, \quad \forall k \quad (33)$$

$$s_k^{\text{oil},1} + s_k^{\text{oil},2} = 1 - \rho_k, \quad \forall k \quad (34)$$

$$x_{ij}, y_{ij}, z_{jk} \geq 0, r_{ij} \in \{0, 1\}, \quad \forall i, j, k, l, w \quad (35)$$

2.2.4. Objective. The optimization objective is to maximize the annualized profit related to biomass-derived chemical and fuel production:

$$\begin{aligned} \max \text{PROFIT} = & \cos T_t^{\text{Revenue}} - \cos T^{\text{VarOper}} - \cos T^{\text{FixOper}} \\ & - \cos T^{\text{Collect}} - \cos T^{\text{Trans}} \\ & - \cos T^{\text{AnnualCapital}} \end{aligned} \quad (36)$$

The PROFIT is a function of the annual revenue ($\text{COST}_t^{\text{Revenue}}$), annual variable operating cost ($\text{COST}^{\text{VarOper}}$), annual fixed operating cost ($\text{COST}^{\text{FixOper}}$), annual biomass collection cost ($\text{COST}^{\text{Collect}}$), annual biomass transportation cost ($\text{COST}^{\text{Trans}}$), and the plant capital cost ($\text{COST}^{\text{AnnualCapital}}$).

The annual revenue $\text{COST}_t^{\text{Revenue}}$ is the sum of the revenue from chemicals, hydrogen, gasoline, and diesel fuel sold all the individual plant locations as described in eq 37. The purchased hydrogen cost is deducted from the total revenues.

$$\begin{aligned} \cos T_t^{\text{Revenue}} = & \sum_{j=1}^J p_k^{\text{char}} c^{\text{char}} + \sum_{k=1}^K \sum_{w=1}^W p_{kw}^{\text{chem}} c_w^{\text{chem}} \\ & + \sum_{k=1}^K (p_k^{\text{excesshydro},1} c^{\text{hydro}} + p_k^{\text{excesshydro},2} c^{\text{hydro}} \\ & + p_k^{\text{lignin}} c^{\text{lignin}} + p_k^{\text{gaso},1} c^{\text{gaso}} + p_k^{\text{gaso},2} c^{\text{gaso}} \\ & + p_k^{\text{diesel},1} c^{\text{diesel}} + p_k^{\text{diesel},2} c^{\text{diesel}}) \\ & - \sum_{k=1}^K (p_k^{\text{mchanthydro},1} c^{\text{hydro}} \\ & + p_k^{\text{mchanthydro},2} c^{\text{hydro}} + p_k^{\text{mchanthydro},3} c^{\text{hydro}}) \end{aligned} \quad (37)$$

The annual variable operating cost $\text{COST}^{\text{VarOper}}$ is the sum of the variable operating costs for all of the operating facilities, which is shown in eq 38. The variable operating costs include the costs for plant operation, such as electricity, process water,

and catalysts. The variable operating costs are derived from previous techno-economic analysis.^{11–14}

$$\begin{aligned} \cos T^{\text{VarOper}} = & \sum_i^I \sum_j^J x_{ij} c_j^{\text{VPyro}} + \sum_i^I \sum_j^J y_{ij} c_j^{\text{VPyro2}} \\ & + \sum_k^K c_k^{\text{VAueReform}} p_k^{\text{aqu}} f_k^{\text{aqu},1} \\ & + \sum_{k=1}^K c_k^{\text{VChem}} p_k^{\text{aqu}} f_k^{\text{aqu},2} \\ & + \sum_{k=1}^K c_k^{\text{VInsoluHydropro}} p_k^{\text{insol}} f_k^{\text{insol},2} \\ & + \sum_{k=1}^K c_k^{\text{VOilReform}} p_k^{\text{oil}} f_k^{\text{oil},1} \\ & + \sum_{k=1}^K c_k^{\text{VOilHydropro}} p_k^{\text{oil}} f_k^{\text{oil},2} \end{aligned} \quad (38)$$

The annual biomass collection cost $\text{COST}^{\text{Collect}}$ is the sum of collection costs for raw biomass and roadside chipped biomass given in eq 39.

$$\cos T^{\text{Collect}} = \sum_{i=1}^I \sum_{j=1}^J x_{ij} c_i^{\text{CR}} + \sum_{i=1}^I \sum_{j=1}^J y_{ij} c_i^{\text{CC}} \quad (39)$$

The annual biomass transportation cost $\text{COST}^{\text{Trans}}$ includes the transportation costs of all of the biomass and bio-oil, as shown in eq 40.

$$\begin{aligned} \cos T^{\text{Trans}} = & \sum_{i=1}^I \sum_{j=1}^J x_{ij} c^{\text{TR}} \tau d_{ij} + \sum_{i=1}^I \sum_{j=1}^J y_{ij} c^{\text{TC}} \tau d_{ij} \\ & + \sum_{k=1}^K \sum_{j=1}^J z_{jk} c^{\text{TOil}} \tau d_{jk} \end{aligned} \quad (40)$$

The plant capital cost, the sum of capital investment for all of the facilities, is calculated on the annual year basis.

$$\begin{aligned} \cos T^{\text{Capital}} = & \left(\sum_{j=1}^J \sum_{l=1}^L \eta_{jl} c_l^{\text{Pyro}} + \sum_{k=1}^K c_k^{\text{OilReform}} + \sum_{k=1}^K c_k^{\text{Chem}} \right. \\ & + \sum_{k=1}^K c_k^{\text{OilHydropro}} + \sum_{k=1}^K c_k^{\text{InsolubleHydropro}} \\ & \left. + \sum_{k=1}^K c_k^{\text{AueReform}} \right) \end{aligned} \quad (41)$$

$$\cos T^{\text{AnnualCapital}} = \frac{\text{int}(1 + \text{int})^t}{(1 + \text{int})^{t-1}} \cos T^{\text{Capital}} \quad (42)$$

A scale factor of $n = 0.6$ is employed to estimate the capital costs.³⁵ In eq 43, S_{new} and S_0 represent the new plant size and the reference plant size, and C_{new} and C_0 are the capital costs for the new plant and the reference plant.

$$C_{\text{new}} = C_0 \left(\frac{S_{\text{new}}}{S_0} \right)^n \quad (43)$$

To reduce the computation time, the capital costs of $c_k^{\text{OilReform}}$, c_k^{Chem} , $c_k^{\text{OilHydropro}}$, $c_k^{\text{InsolubleHydropro}}$, and $c_k^{\text{AueReform}}$ are

linearized. For $c_k^{\text{OilReform}}$ calculation, the binary variable $\mu_{dk}^{\text{OilReform}}$ is introduced. $\mu_{dk}^{\text{OilReform}}$ is equal to one if the bio-oil mass flow at location k is in the disjunctive segment d . The bio-oil mass flow can only exist in one segment.

$$\sum_{d=1}^D \mu_{dk}^{\text{OilReform}} = 1, \quad \forall k \quad (44)$$

The continuous variables are different for each disjunctive segment d . The bio-oil flow and capital cost are presented as

$$p_k^{\text{oil}} f_k^{\text{oil},1} = \sum_{d=1}^D p_{dk}^{\text{OilReform}}, \quad \forall k \quad (45)$$

$$c_k^{\text{OilReform}} = \sum_{d=1}^D c_{dk}^{\text{OilReform,disjunct}}, \quad \forall k \quad (46)$$

In eq 46, here $c_{dk}^{\text{OilReform,disjunct}}$ represents the bio-oil reforming to hydrogen capital cost in segment d at location k . It has a linear relation with the bio-oil mass flow, which is illustrated in eq 47. Here $a_d^{\text{OilReform}}$ and $b_d^{\text{OilReform}}$ are the coefficient for the linearized capital cost.

$$\begin{aligned} c_{dk}^{\text{OilReform,disjunct}} = & a_d^{\text{OilReform}} \mu_{dk}^{\text{OilReform}} + b_d^{\text{OilReform}} p_{dk}^{\text{OilReform}}, \\ & \forall k, \forall d \end{aligned} \quad (47)$$

$$p_d^{\text{Min,OilReform}} \leq p_{dk}^{\text{OilReform}} \leq p_d^{\text{Max,OilReform}}, \quad \forall k, \forall d \quad (48)$$

$$p_{dk}^{\text{OilReform}} \geq 0, \quad \forall k, \forall d \quad (49)$$

$$c_{dk}^{\text{OilReform,disjunct}} \geq 0, \quad \forall k, \forall d \quad (50)$$

$$\mu_{dk}^{\text{OilReform}} \in \{0, 1\}, \quad \forall k, \forall d \quad (51)$$

Using the same methodology, c_k^{Chem} , $c_k^{\text{OilHydropro}}$, $c_k^{\text{InsolubleHydropro}}$, and $c_k^{\text{AueReform}}$ are all linearized.

Aqueous phase reforming to chemicals facility:

$$\sum_{d=1}^D \mu_{dk}^{\text{chem}} = 1, \quad \forall k \quad (52)$$

$$p_k^{\text{aqu}} f_k^{\text{aqu},2} = \sum_{d=1}^D p_{dk}^{\text{chem}}, \quad \forall k \quad (53)$$

$$c_k^{\text{chem}} = \sum_{d=1}^D c_{dk}^{\text{chem,disjunct}}, \quad \forall k \quad (54)$$

$$c_{dk}^{\text{chem,disjunct}} = a_d^{\text{chem}} \mu_{dk}^{\text{chem}} + b_d^{\text{chem}} p_{dk}^{\text{chem}}, \quad \forall k, \forall d \quad (55)$$

$$p_d^{\text{Min,chem}} \leq p_{dk}^{\text{chem}} \leq p_d^{\text{Max,chem}}, \quad \forall k, \forall d \quad (56)$$

$$p_{dk}^{\text{chem}} \geq 0, \quad \forall k, \forall d \quad (57)$$

$$c_{dk}^{\text{chem,disjunct}} \geq 0, \quad \forall k, \forall d \quad (58)$$

$$\mu_{dk}^{\text{chem}} \in \{0, 1\}, \quad \forall k, \forall d \quad (59)$$

Bio-oil hydroprocessing to liquid fuels facility:

$$\sum_{d=1}^D \mu_{dk}^{\text{OilHydropro}} = 1, \quad \forall k \quad (60)$$

$$p_k^{oil, f_{oil,2}} = \sum_{d=1}^D p_{dk}^{OilHydropro}, \quad \forall k \quad (61)$$

$$c_k^{OilHydropro} = \sum_{d=1}^D c_{dk}^{OilHydropro, disjunct}, \quad \forall k \quad (62)$$

$$c_{dk}^{OilHydropro, disjunct} = a_d^{OilHydropro} \mu_{dk}^{OilHydropro} + b_d^{OilHydropro} p_{dk}^{OilHydropro}, \quad \forall k, \forall d \quad (63)$$

$$p_d^{Min, OilHydropro} \leq p_{dk}^{OilHydropro} \leq p_d^{Max, OilHydropro}, \quad \forall k, \forall d \quad (64)$$

$$p_{dk}^{OilHydropro} \geq 0, \quad \forall k, \forall d \quad (65)$$

$$c_{dk}^{OilHydropro, disjunct} \geq 0, \quad \forall k, \forall d \quad (66)$$

$$\mu_{dk}^{OilHydropro} \in \{0, 1\}, \quad \forall k, \forall d \quad (67)$$

Water-insoluble phase hydroprocessing to liquid fuels:

$$\sum_{d=1}^D \mu_{dk}^{InsolHydropro} = 1, \quad \forall k \quad (68)$$

$$p_k^{insol, f_{insol,2}} = \sum_{d=1}^D p_{dk}^{InsolHydropro}, \quad \forall k \quad (69)$$

$$c_k^{InsolHydropro} = \sum_{d=1}^D c_{dk}^{InsolHydropro, disjunct}, \quad \forall k \quad (70)$$

$$c_{dk}^{InsolHydropro, disjunct} = a_d^{InsolHydropro} \mu_{dk}^{InsolHydropro} + b_d^{InsolHydropro} p_{dk}^{InsolHydropro}, \quad \forall k, \forall d \quad (71)$$

$$p_d^{Min, InsolHydropro} \leq p_{dk}^{InsolHydropro} \leq p_d^{Max, InsolHydropro}, \quad \forall k, \forall d \quad (72)$$

$$p_{dk}^{InsolHydropro} \geq 0, \quad \forall k, \forall d \quad (73)$$

$$c_{dk}^{InsolHydropro, disjunct} \geq 0, \quad \forall k, \forall d \quad (74)$$

$$\mu_{dk}^{InsolHydropro} \in \{0, 1\}, \quad \forall k, \forall d \quad (75)$$

Aqueous phase reforming to hydrogen facility:

$$\sum_{d=1}^D \mu_{dk}^{AquReform} = 1, \quad \forall k \quad (76)$$

$$p_k^{aqu, f_{aqu,1}} = \sum_{d=1}^D p_{dk}^{AquReform}, \quad \forall k \quad (77)$$

$$c_k^{AquReform} = \sum_{d=1}^D c_{dk}^{AquReform, disjunct}, \quad \forall k \quad (78)$$

$$c_{dk}^{AquReform, disjunct} = a_d^{AquReform} \mu_{dk}^{AquReform} + b_d^{AquReform} p_{dk}^{AquReform}, \quad \forall k, \forall d \quad (79)$$

$$p_d^{Min, AquReform} \leq p_{dk}^{AquReform} \leq p_d^{Max, AquReform}, \quad \forall k, \forall d \quad (80)$$

$$p_{dk}^{AquReform} \geq 0, \quad \forall k, \forall d \quad (81)$$

$$c_{dk}^{AquReform, disjunct} \geq 0, \quad \forall k, \forall d \quad (82)$$

$$\mu_{dk}^{AquReform} \in \{0, 1\}, \quad \forall k, \forall d \quad (83)$$

The annual fixed operating cost $COST^{FixOper}$ is defined as a sum of a factor 0.035 of capital cost and 60% of salaries (eq 84). The fixed operating cost includes insurance and taxes, overhead, and maintenance costs. The overhead fee is assumed to be 60% of the total labor salaries. The maintenance costs and insurances are assumed to be 2% and 1.5% of the total fixed capital investment (TPI), respectively.³⁶

$$\cos T^{FixOper} = 0.035 \cos T^{AnnualCapital} + 0.6 \cos T^{Salaries} \quad (84)$$

This mixed-integer nonlinear programming (MINLP) model employs MATLAB³⁷ to collect the data and uses geographic information system (GIS) software to map the biomass availability and locations. The mathematical model is solved using GAMS/DICOPT linked with MINLP solver.³⁸ The optimization model has 144 877 nonzero elements, 14 802 single equations and 3828 discrete variables, and 37 508 single variables. To simplify the model, some linearization of equations are adopted (see section 2.2.4). For some extreme cases, the running would take up to ~30 h.

3. BASE STUDY

3.1. Data Sources. In this case study, forest residue from counties in Minnesota are the selected feedstock. The amount of available forest residue per county was obtained from the National Renewable Energy Laboratory³⁹ as shown in Figure 2.

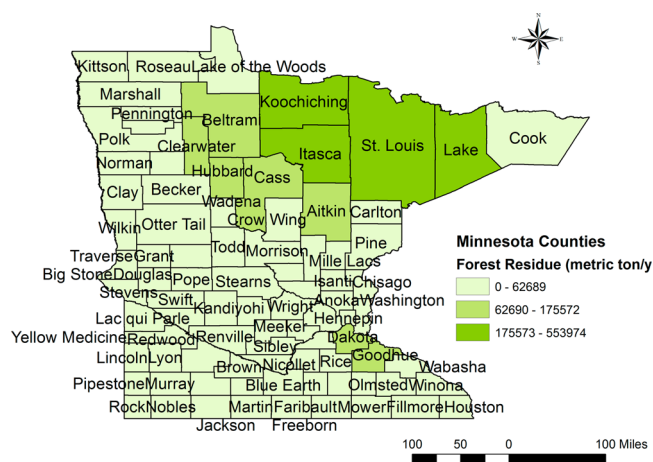


Figure 2. Forest residue availability in U.S. and Minnesota.

It is assumed that all of the forest residue could be collected for biorefinery. The state of Minnesota has the most abundant forest residue in the Midwest. In this paper, each county in Minnesota is considered as a candidate harvesting site, a potential fast pyrolysis facility location, and potential biorefinery facility location.

The collection costs for raw biomass and roadside chipped biomass are based on Leinonen.⁴⁰ Forest haulage cost is \$10.8/metric for raw forest residue. The stumpage price for the forest residue is assumed to be \$5/metric ton. So, the collection cost for raw biomass is \$15.8/metric ton. For roadside chipped forest residue, there is a \$10.8/metric ton haulage

cost, \$10.8/metric chipping cost, and stumpage cost of \$5/metric ton. Therefore, the collection cost for roadside chipped forest residue is \$26.6/metric ton.

The costs of different harvesting methods for forest residues have also been reported by Leinonen.⁴⁰ The four harvest methods include bundle, terrain chip, road chip, and plant chip. The road transportation costs for raw forest residue and roadside chipped forest residue are \$12.8/ton and \$18.3/ton for 80 km. As calculated from this information, the variable transportation costs for raw forest residue and roadside chipped forest residue are assumed to be \$0.41/metric-ton-mile and \$0.28/metric-ton-mile. The transportation cost of bio-oil is assumed to be same as the national average truck shipping cost of \$0.287/metric-ton-mile.⁴¹ The distances between counties are based on the great circle distances calculated using the latitudes and longitudes of the county centers. Tortuosity factors are incorporated to estimate the actual transportation distances. The tortuosity factors are assumed to be 1.27 for truck.⁴²

Publicly reported product yields and prices are given in Table 1. Here we assume the received forest residue is 3333 metric ton/day with 40% moisture. The bio-oil yield is 1306 metric ton/day and the char yield is 159 metric ton/day which is adjusted based on the original Aspen Plus model.¹¹ The yield data for bio-oil conversion, aqueous phase conversion, and insoluble phase conversion are collected based on the Aspen Plus model reported in previous studies.^{11–14} The product prices are collected from previous techno-economic analysis and online databases.^{12,28,43} The lignin price is assumed equal to the char price based on their use in heating applications. Gasoline and diesel prices are assumed to be \$3.25/gallon and \$3.99/gallon (based on Minnesotagasprices.com, accessed in 2013⁴⁴). Hydrogen price is assumed to be \$2/kg. The range of hydrogen and liquid fuel prices will be investigated in this paper.

Seven capacity levels (L1, L2, L3, L4, L5, L6, and L7) are considered for fast pyrolysis facilities; L1, L2, L3, L4, L5, L6, and L7 correspond to 100, 200, 500, 1000, 2000, 4000, and 8000 metric ton/day dry biomass processing capacities. The 2000 metric ton/day capacity plant is selected as the reference plant. The economies of scale power law and a scaling factor of 0.6 are used to calculate the capital costs for different capacity levels.^{35,45} The capital costs for the fast pyrolysis facilities are based on previous techno-economic analysis.^{12,14,43} The variable operating costs for raw biomass fast pyrolysis and roadside chipped biomass fast pyrolysis are \$13.97 and \$12.93 per metric ton, respectively.

For biorefinery facilities, the capital costs are linearized based on the reference capital costs. The reference capital costs and variable operating cost for various biorefinery facilities are presented in Table 2.

Based on the reference data, the biorefinery facility capital costs are calculated. The linearized relations between mass flows and capital costs for various biorefinery facilities are shown in the Supporting Information. Here, the mass flows are divided into five segments and the corresponding mass flow ranges for the biorefinery facilities are shown in the Supporting Information.

3.2. Base Case Results and Discussion. The MINLP model is developed to determine the product distribution, optimal capacities, and locations of the fast pyrolysis and biorefinery facilities in Minnesota by maximizing the annual profit. The optimal locations for the fast pyrolysis and

Table 1. Product Prices and Yields from Biomass and Bio-Oil Conversion Processes

	Yield of As-Received Wet Biomass	Price (\$/metric ton)
bio-oil	0.39	
char	0.0456 ^a	18.21 [14]
	Yield from Bio-Oil Conversion	Price (\$/metric ton)
water-insoluble phase(lignin)	0.3449 ^a	18.21
aqueous phase	0.656 ^a	
hydrogen from whole bio-oil reforming	0.123 [11]	2000
gasoline from whole bio-oil hydroprocessing	0.19 [13]	1307
diesel fuel yield from whole bio-oil hydroprocessing	0.25 [13]	1238
hydrogen need for whole bio-oil hydroprocessing	0.04 [12]	2000
Chemicals	Yield from Aqueous Phase [14] ^b	Price (\$/metric ton) [28]
ethylene	0.068	1296.8
propylene	0.11	1513.6
butylene	0.03	750
benzene	0.022	1279.8
toluene	0.04	1067.9
xylene	0.016	1105.4
ethylbenzene	0.002	1270
styrene	0.0012	850
indene	0.0004	850
naphthalene	0.0004	850
hydrogen production from aqueous phase reforming	0.092	2000
hydrogen input for chemical synthesis	0.02	2000
	Yield of Water-Insoluble Phase	Price (\$/metric ton)
gasoline from water-insoluble phase	0.19 [13]	1307
diesel fuel from water-insoluble phase	0.25 [13]	1238
hydrogen need for water-insoluble bio-oil hydroprocessing	0.04 [12]	2,000

^aAdjusted based on the Aspen Plus model of the pyrolysis reforming pathway in ref 11. ^bAdjusted based on the Aspen Plus model of the pyrolysis chemicals pathway in ref 14.

biorefinery locations are illustrated in Figure 3. The results predict that six fast pyrolysis facilities (including the preprocessing facilities) and one biorefinery facility would be built in the state of Minnesota. The model employs 42 counties to supply raw biomass and 35 counties are selected to supply roadside chipped biomass. There is a trade-off between the increased roadside chipped biomass collections cost and reduced transportation cost. The roadside chipped biomass supply sites are farther than raw biomass supply sites for each fast pyrolysis facility.

The Northern Minnesota region has the most abundant forest residue sources, especially in Lake, Itasca, St. Louis, Koochiching, Cass, Aitkin, Hubbard, Clearwater, and Beltrami Counties. The forest residue in those nine counties represents 70% of the total forest residue in Minnesota. The six fast pyrolysis facilities are built in St. Louis, Koochiching, Clear Water, Aitkin, Dakota and Winona. Among these counties, St. Louis County has the largest amount of forest residue, representing approximately 19% of the total forest residue in Minnesota. So in St. Louis County, a fast pyrolysis facility with the capacity of 2000 metric ton/day is built. Two fast pyrolysis

Table 2. Facility Design, Biomass Mass Flow, Capital, And Operating Cost Reference Data for Biorefinery Facilities

facility	bio-oil mass flow (metric ton/day)	capital cost (\$MM) ^a	variable operating cost (\$/metric ton bio-oil)	reference
bio-oil reforming to hydrogen	1306	\$125	12.74	[11]
bio-oil hydroprocessing to gasoline and diesel fuel	1650.4	\$170	34.36	[13]
aqueous phase bio-oil to chemicals	822	\$55	10.19	[14]
aqueous phase bio-oil to hydrogen	857	\$120	15.18	[14]
water-insoluble bio-oil hydroprocessing to gasoline and diesel fuel	1650.4	\$170	34.36	[13]

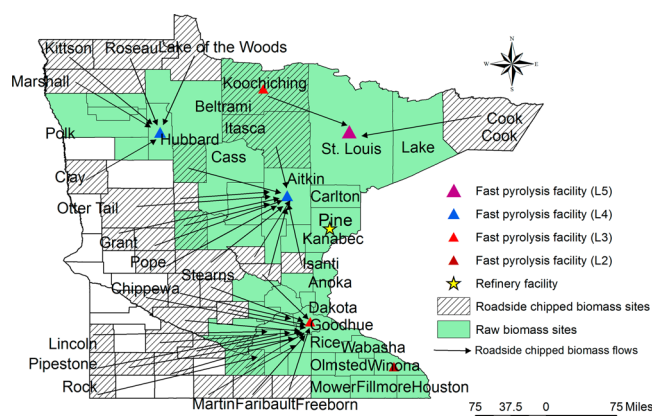
^aAdjusted to \$US 2013.

Figure 3. Optimal fast pyrolysis and (bio) refinery facility locations, and their biomass distribution network in Minnesota.

facilities with capacity of L4 (1000 metric ton/day) are built in Hubbard and Aitkin. Two fast pyrolysis facilities are built in Koochiching and Dakota with capacity of L3 (500 metric ton/day). A 200 metric ton/day fast pyrolysis facility is proposed to be built in Winona. The biomass in bottom area of Minnesota is collected and transported to Dakota County for bio-oil production. The biorefinery facility is built in Pine County and it receives the transported bio-oil from all of the fast pyrolysis facilities. In biorefinery facility, bio-oil is phase separated. The water-soluble phase bio-oil is totally consumed to produce commodity chemicals and the water-insoluble phase is employed to produce gasoline and diesel fuel. The required hydrogen is purchased from merchant sources. Although merchant hydrogen is not widely marketed to biorefineries, the wide availability of low cost natural gas and renewable electricity (wind and solar) suggests that hydrogen could be available given sufficient demand.⁴⁶

The total generated bio-oil is 1.1 million metric ton per year and the total annualized cost is \$330 million. Among all of the costs, the facility capital cost is the largest expenditure, representing 31% of the total cost. The production cost includes fixed operating costs (9%) and variable operating costs (21%). The remainder of the annual cost consists of biomass collection and transportation expenses, which are 14% and 25% of the total, respectively. The transportation expenditures include the costs of transporting the raw biomass, road chipped biomass, and bio-oil. The raw biomass transportation is the largest among them, representing 18% of the total cost.

4. SENSITIVITY ANALYSIS

The market prices for final products have strong impacts on the product distribution and optimal facility locations. In this section, the effects of hydrogen, liquid fuels, and chemicals prices on the annualized profit are investigated. They are assumed to

be independent of each other and vary from 25% to 200% of the baseline prices.

4.1. Effects of Hydrogen and Liquid Fuel Prices on Annualized Profits. The annualized profit relationship to the hydrogen and liquid fuel prices using the baseline chemicals price is shown in Figure 4. Figure 4a is the 3D plot of

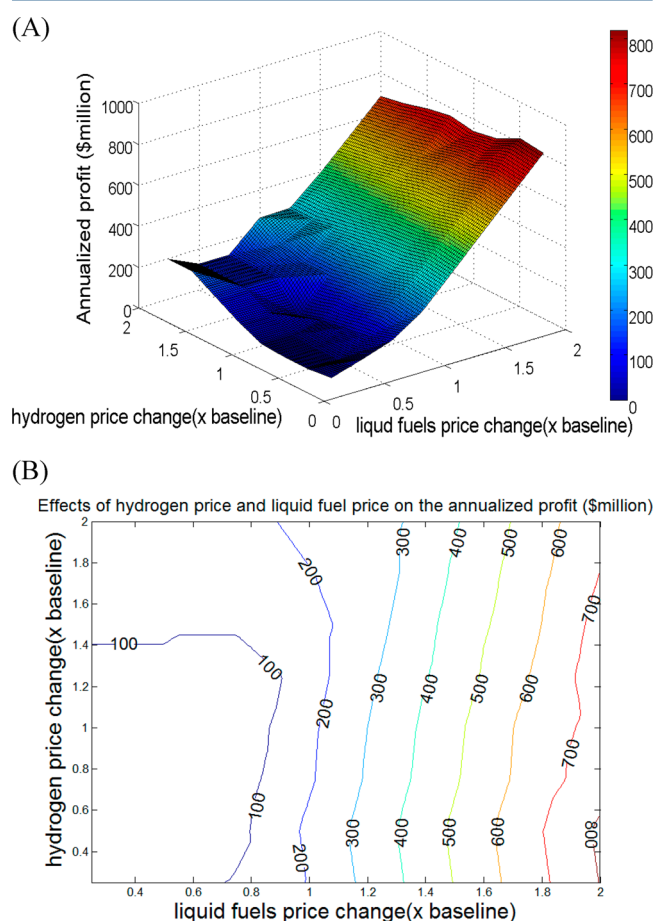


Figure 4. Effects of hydrogen price and liquid fuel price using baseline chemical prices on the annualized profit (\$million).

annualized profit as a function of hydrogen and liquid fuel prices. Figure 4b is the contour plot for the annualized profit as a function of hydrogen and liquid fuels prices. As it describes, when the liquid fuel price is larger than the baseline price, the contour lines are monotonic which means the increase of hydrogen price would reduce the annualized profit. When the liquid fuels price is smaller than or equal to the baseline price, the contour lines are not monotonic which means there would be a fluctuation for annualized profit when the hydrogen or liquid fuels price changes. As shown, the annualized profit

increases from a negligible profit to more than \$800 million with a 200% increase in the liquid fuel price. A similar hydrogen price increase adds less than \$200 million to the annualized profit.

Figure 5 shows the correlations of hydrogen price with the annualized profit using baseline chemical and liquid fuel prices.

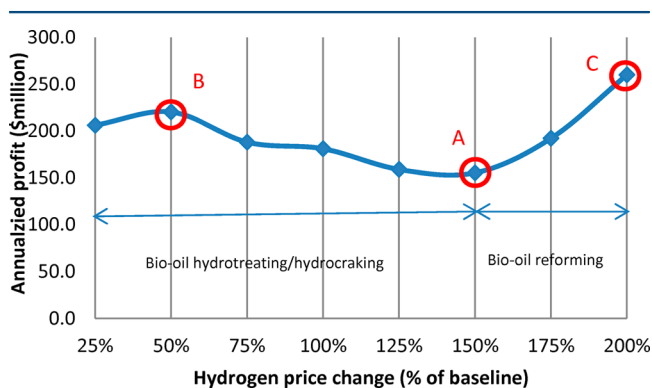


Figure 5. Effects of varying hydrogen price on the annualized profit. Points A, B, and C indicate turning points in biorefinery operation strategy.

It shows that the annualized profit is reduced first and then increases along with the increase of hydrogen price.

When hydrogen price is \$3/kg (point A), two fast pyrolysis facilities are built in Beltrami and Dakota County with capacities of L3 and one fast pyrolysis facility is built in St. Louise with a capacity of L6. All the bio-oil produced from fast pyrolysis is transported to the biorefinery facility that is located in St. Louis. In the biorefinery facility, liquid fuels (gasoline and

diesel) are produced through hydrotreating/hydrocracking of bio-oil. The annualized profit for point A is \$155 million. When the hydrogen price is \$1/kg (point B), then the annualized profit is \$220 million. Five fast pyrolysis facilities are built in Clearwater (L5), Dakota (L3), Koochiching (L3), St. Louis (L5) and Winona (L2), respectively. All of the bio-oil is transported from the fast pyrolysis facilities to the biorefinery facility that is built in Mahanomen County. Point A (\$3/kg hydrogen price) is a strategy turning point. When the hydrogen price is less than \$3/kg, liquid fuels are selected as the refinery products and hydrogen is purchased from a merchant instead of from on-site production. All of the liquid fuels are produced from the whole bio-oil hydrotreating. Higher hydrogen prices correspond with higher operating costs. So when the hydrogen price is less than \$3/kg, the annualized profit would decrease along with the increase of the hydrogen price.

When the hydrogen price is \$4/kg (Point C), the annualized profit is \$260 million. Four fast pyrolysis facilities are built in Dakota (L3), Itasca (L6), Lake (L3), and Olmsted (L2), respectively. From point A to point C, all of the bio-oil is catalytically reformed to produce hydrogen. Because hydrogen is selected as the final product from point A to point C, the annualized profit increases along with the increase of hydrogen price if the hydrogen sales prices is greater than \$3/kg. Compared to point A and B, there is no consumption of roadside chipped biomass for point C. In addition, the biomass collection area is smaller than that of point A and point B. This is because hydrogen price is much higher for point C so a smaller collection and conversion of biomass for point C could achieve the same level of profit for point B and C. The optimal locations of facilities and biomass supplies for point A, B, and C are shown in the Supporting Information.

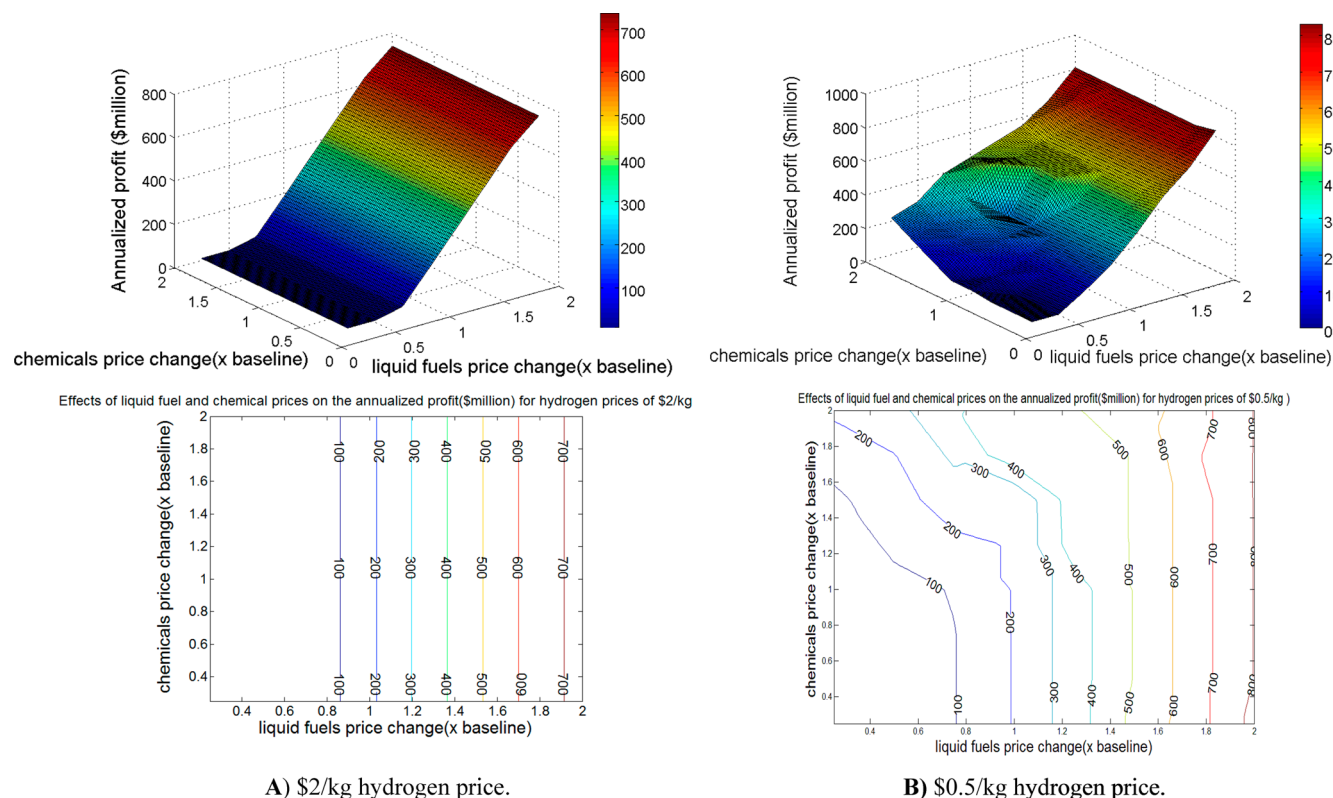


Figure 6. Effects of liquid fuel and chemical prices on the annualized profit for hydrogen prices of \$2/kg (A) and \$0.5/kg (B).

4.2. Effects of Chemicals and Liquid Fuel Prices on the Annualized Profit. Figure 6 shows the effects of chemicals and liquid fuel prices on the annualized profit using two hydrogen prices (\$2/kg and \$0.5/kg). In Figure 6a, the hydrogen price is \$2/kg and in Figure 6b, the hydrogen price is \$0.5/kg. When the hydrogen price is \$2/kg, the contour lines are parallel to each other and the annualized profit would not change along with the chemicals prices at a fixed liquid fuels price. There is no profit if liquid fuels price is smaller than 75% of the baseline price and the change of chemicals price on a 25%–200% basis would not affect the annualized profit with the fixed liquid fuels price.

When the liquid fuels price is at 75% of baseline, there are five fast pyrolysis facilities that are built in Dakota (L3), Koochiching (L3), Aitkin (L4), Clearwater (L4), and St. Louis (L5). All of the bio-oil produced from fast pyrolysis facilities are transported to the refinery facility located in Pine. The optimal locations of facilities and biomass supplies are shown in the Supporting Information for the case scenario when the liquid fuels price is 75% of its baseline value.

For hydrogen price is \$0.5/kg (Figure 6b), the contour lines are almost parallel to the y -axis if the liquid fuels prices are above the 125% of the baseline liquid fuels price. This indicates that chemicals price almost have no role on the annualized profit at higher liquid fuels price ($>125\%$ baseline liquid fuels price). While the liquid fuels price is below 125% of the baseline price, the contour lines would change which means there is the trade-off between chemicals production and transportation fuels production.

Figure 7 shows the correlations of liquid fuels prices with the annualized profit using the baseline chemicals price with

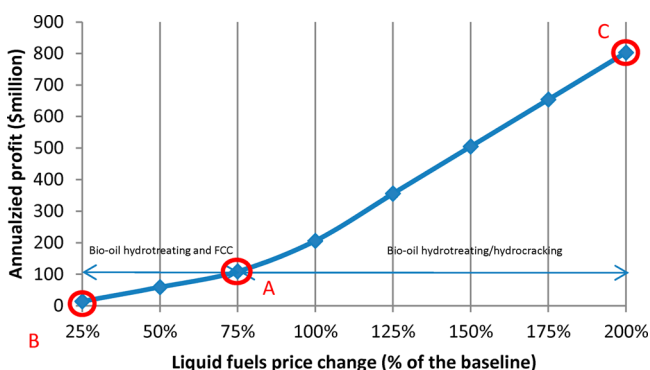


Figure 7. Effect of liquid fuel prices on the annualized profit (H2: \$0.5/kg, baseline chemicals price) and biorefinery operation strategies, Bio-oil hydrotreating and FCC (A,B) and bio-oil hydrotreating/hydrocracking (B,C).

\$0.5/kg of hydrogen. Point A is a switching point. When the liquid fuels prices are below or equal to 75% of the baseline prices, chemicals facility is selected as the bio-oil upgrading facility. When the liquid fuel prices are larger than 75% of the baseline, all the bio-oil is hydroprocessed to liquid fuels. The annualized profit would grow along with the increase of the hydrocarbon fuel price. At point A, four fast pyrolysis facilities are built to process the biomass. Two fast pyrolysis facilities are built in Dakota and Koochiching with capacities of L3. Two fast pyrolysis facilities are built in Clearwater and St. Louis with capacities of L5. All of the bio-oil is transported to the biorefinery facility in Mahnommen where the bio-oil is converted to commodity chemicals through two-stage hydrotreating

and fluid catalytic cracking (FCC) process. When at point B, there is one fast pyrolysis built in Clearwater, St. Louis, and Koochiching with Level 5, Level 4, and Level 3, respectively. The bio-oil upgrading facility is built in Mahnommen in which the transported bio-oil from fast pyrolysis facilities is converted into commodity chemicals. For point C, six fast pyrolysis facilities are built in Fillmore (L2), Dakota and Koochiching (L3), Clearwater and CrowWing (L4), and St. Louis (L5), respectively. The optimal locations of facilities and biomass supplies for points A, B, and C are shown in the Supporting Information. All of the bio-oil are transported to the upgrading facility (Yellow Medicine County) and converted to liquid fuels. The optimal locations of facilities and biomass supplies for point A, B, and C are shown in the Supporting Information.

5. CONCLUSION

This paper investigates the product selection along with the optimal production planning and facility locations for biomass fast pyrolysis and biorefinery facilities using a MINLP model. Decisions on selection of technologies (including catalytic reforming, hydrotreating/hydrocracking, hydrotreating/FCC), and upgraded products (including commodity chemicals, lignin, char, hydrogen, and gasoline diesel) can be recommended through this model for Minnesota State as a case study. The results show that the harvest sites rich in biomass resources are the preferable locations for building fast pyrolysis facilities. Compared to the upgrading of phase separated bio-oil, whole bio-oil upgrading is preferable in terms of economic costs. Hydrogen and liquid fuel prices have greater influence on the annualized profit than the commodity chemical price.

These findings can help inform the decision-making process of a fast pyrolysis facility site selection and operation. The optimal locations identified in this study would be of interest to any biorefinery enterprise seeking to convert forest residues in Minnesota. The effects of hydrogen, chemicals, and liquid fuel prices on the annualized profits could signal future opportunities for investing in facilities based on the proposed technology configurations.

■ ASSOCIATED CONTENT

Supporting Information

Total capital costs for fast pyrolysis facilities with various biomass input capacities are provided in Table S1. Linearized capital costs of biorefineries vs facility bio-oil input capacity are based on the segments shown in Table S2. Figure S1 provides linearized capital costs of biorefineries versus facility bio-oil input capacity. Figures S2–S8 provide the optimal locations, types, and sizes of facilities for various points (Points A, B, and C) in Figure 5–7. This material is available free of charge via the Internet at <http://pubs.acs.org>.

■ AUTHOR INFORMATION

Corresponding Author

*M. M. Wright. Tel: +1-515-294-0913. E-mail: markmw@iastate.edu

Present Address

†National Bioenergy Center, National Renewable Energy Laboratory, 1617 Cole Boulevard, Golden, CO 80401, USA

Notes

The authors declare no competing financial interest.

ACKNOWLEDGMENTS

The authors acknowledge the financial support of the Bioeconomy Institute and the Biobased Industry Center of Iowa State University.

NOMENCLATURE

Subscripts

- i = Biomass candidate harvest locations, 1, 2, ..., I
- j = Candidate fast pyrolysis facility locations, 1, 2, ..., J
- k = Candidate biorefinery facility locations, 1, 2, ..., K
- l = Allowed fast pyrolysis facility capacity levels, 1, 2, ..., L
- w = Chemicals species, 1, 2, ..., M
- d = Segments for capital linearization, 1, 2, ..., D

Decision Variables

- r_{ij} = If a fast pyrolysis facility of capacity level l exists in candidate facility location j , binary
- ρ_k = Bio-oil phase separation exists in biorefinery candidate facility location k , binary
- $\mu_{dk}^{\text{AqueReform}}$ = Aqueous phase bio-oil reforming capacity at location k exist in segment d , binary
- μ_{dk}^{chem} = Chemicals capacity at location k exist in segment d , binary
- $\mu_{dk}^{\text{InsolHydropro}}$ = Insoluble phase hydroprocessing capacity at location k exist in segment d , binary
- $\mu_{dk}^{\text{OilHydropro}}$ = Bio-oil hydroprocessing capacity at location k exist in segment d , binary
- $\mu_{dk}^{\text{OilReform}}$ = Bio-oil reforming capacity at location k exist in segment d , binary
- x_{ij} = Amount of raw chipped biomass transported from harvest location i to fast pyrolysis facility location j , metric ton/year
- y_{ij} = Amount of roadside chipped biomass transported from harvest location i to fast pyrolysis facility location j , metric ton/year
- z_{jk} = Amount of bio-oil transported from fast pyrolysis facility location j to biorefinery facility location k , metric ton/year
- F_i = Total amount of transported biomass from harvest location i to other locations, metric ton/year
- B_j = Total amount of transported biomass from harvest locations to the fast pyrolysis facility location j , metric ton/year
- H_j = Total amount of bio-oil from the fast pyrolysis facility location j , metric ton/year
- T_k = Total amount of bio-oil for biorefinery facility location k , metric ton/year
- p_j^{char} = Total generated char in fast pyrolysis location j , metric ton/year
- p_k^{aqu} = Total generated aqueous phase bio-oil in biorefinery location k , metric ton/year
- p_k^{insol} = Total generated water-insoluble phase bio-oil in biorefinery location k , metric ton/year
- $f_k^{\text{aqu},1}$ = Split ratio of aqueous phase for hydrogen production in biorefinery location k
- $f_k^{\text{aqu},2}$ = Split ratio of aqueous phase for chemicals production in biorefinery location k
- $p_k^{\text{hydro},1}$ = Total produced hydrogen from aqueous phase reforming in biorefinery location k , metric ton/year
- p_{kw}^{chem} = Total produced chemical w in biorefinery location k , metric ton/year
- $n_k^{\text{hydro},1}$ = Required hydrogen for chemicals production in biorefinery location k , metric ton/year
- $p_k^{\text{mechhydro},1}$ = Purchased hydrogen for chemicals production in biorefinery location k , metric ton/year

- $s_k^{\text{aqu},1}$ = Split ratio of hydrogen generated from aqueous phase reforming for chemicals production in biorefinery location k
- $f_k^{\text{insol},1}$ = Split ratio of water-insoluble phase for lignin production in biorefinery location k
- $f_k^{\text{insol},2}$ = Split ratio of water-insoluble phase for hydroprocessing in biorefinery location k
- p_k^{lignin} = Total produced lignin in biorefinery location k , metric ton/year
- $p_k^{\text{gaso},1}$ = Total produced gasoline from water-insoluble phase hydroprocessing in biorefinery location k , metric ton/year
- $p_k^{\text{diesel},1}$ = Total produced diesel fuel from water-insoluble phase hydroprocessing in biorefinery location k , metric ton/year
- $n_k^{\text{hydro},2}$ = Required hydrogen for water-insoluble phase hydroprocessing in biorefinery location k , metric ton/year
- $p_k^{\text{mechhydro},2}$ = Total purchased hydrogen for water-insoluble phase hydroprocessing in biorefinery location k , metric ton/year
- $s_k^{\text{aqu},2}$ = Split ratio of hydrogen generated from aqueous phase reforming for hydroprocessing in biorefinery location k
- $s_k^{\text{aqu},3}$ = Remaining ratio of hydrogen generated from aqueous phase reforming in biorefinery location k
- $p_k^{\text{excesshydro},1}$ = Total excess hydrogen from aqueous phase reforming in biorefinery location k , metric ton/year
- p_k^{oil} = Total unseparated bio-oil generated in biorefinery location k , metric ton/year
- $f_k^{\text{oil},1}$ = Split ratio of bio-oil for hydrogen in biorefinery location k
- $f_k^{\text{oil},2}$ = Split ratio of bio-oil for hydroprocessing in biorefinery location k
- $p_k^{\text{hydro},2}$ = Total produced hydrogen from bio-oil reforming in biorefinery location k , metric ton/year
- $p_k^{\text{gaso},2}$ = Total produced gasoline from bio-oil hydroprocessing in biorefinery location k , metric ton/year
- $p_k^{\text{diesel},2}$ = Total produced diesel fuel from bio-oil hydroprocessing in biorefinery location k , metric ton/year
- $n_k^{\text{hydro},3}$ = Required hydrogen for bio-oil hydroprocessing in biorefinery location k , metric ton/year
- $p_k^{\text{mechhydro},3}$ = Amount of purchased hydrogen, metric ton/year
- $s_k^{\text{oil},1}$ = Split ratio of hydrogen generated from bio-oil reforming for bio-oil hydroprocessing in biorefinery location k
- $s_k^{\text{oil},2}$ = Remaining ratio of hydrogen generated from bio-oil reforming
- $p_k^{\text{excesshydro},2}$ = Total excess hydrogen from bio-oil reforming in biorefinery location k , metric ton/year
- $p_k^{\text{oilReform}}$ = Total bio-oil mass flow for reforming exist in segment d in biorefinery location k , metric ton/year
- $c_{dk}^{\text{OilReform,disjunct}}$ = Capital cost for bio-oil reforming exist in segment d in biorefinery location k , \$
- p_{dk}^{chem} = Total aqueous phase bio-oil mass flow for chemicals production exist in segment d in biorefinery location k , metric ton/year
- $c_{dk}^{\text{chem,disjunct}}$ = Capital cost for chemicals production exist in segment d in biorefinery location k , \$
- $p_{dk}^{\text{OilHydropro}}$ = Total bio-oil mass flow for hydroprocessing exist in segment d in biorefinery location k , metric ton/year
- $c_{dk}^{\text{OilHydropro,disjunct}}$ = Capital cost for bio-oil hydroprocessing exist in segment d in biorefinery location k , \$
- $p_{dk}^{\text{InsolHydropro}}$ = Total water-insoluble bio-oil mass flow for hydroprocessing exist in segment d in biorefinery location k , metric ton/year
- $c_{dk}^{\text{InsolHydropro,disjunct}}$ = Capital cost for water-insoluble bio-oil hydroprocessing exist in segment d in biorefinery location k , \$

$p_{dk}^{\text{AquReform}}$ = Total aqueous phase bio-oil mass flow for reforming exist in segment d in biorefinery location k , metric ton/year
 $c_{dk}^{\text{AquReform,disjunct}}$ = Capital cost for aqueous phase bio-oil reforming exist in segment d in biorefinery location k , \$

Parameters

A_i = Biomass availability in harvest location i , metric ton/year
 F_i = Total collected biomass in harvest location i , metric ton/year
 $\text{Cap}_l^{\text{Pyro}}$ = Capacity level l for the fast pyrolysis facility, metric ton/year
 c_i^{CR} = Unit collection cost for raw biomass in location i , \$/metric ton
 c_i^{CC} = Unit collection cost for roadside chipped biomass in location i , \$/metric ton
 c^{TR} = Unit transportation cost for raw biomass, \$/(metric ton mile)
 c^{TC} = Unit transportation cost for roadside chipped biomass, \$/(metric ton mile)
 c^{TOil} = Unit transportation cost for bio-oil, \$/(metric ton mile)
 d_{ij} = Distance from harvest location i to fast pyrolysis location j , mile
 d_{jk} = Distance from fast pyrolysis preprocessed location j to the biorefinery facility location k , mile
 c_j^{Pyro} = Capital cost for fast pyrolysis facility at capacity level l , \$
 c_j^{VPyro} = Variable operating cost for raw biomass fast pyrolysis at location j , \$/metric ton
 c_j^{VPyro2} = Variable operating cost for roadside chipped biomass fast pyrolysis at location j , \$/metric ton
 $c_k^{\text{VAquReform}}$ = Variable operating cost for aqueous phase reforming facility at location k , \$/metric ton
 c_k^{VChem} = Variable operating cost for chemicals facility at location k , \$/metric ton
 $c_k^{\text{VInsoluHydropro}}$ = Variable operating cost for water-insoluble phase hydroprocessing facility at location k , \$/metric ton
 $c_k^{\text{VOilReform}}$ = Variable operating cost for bio-oil reforming facility at location k , \$/metric ton
 $c_k^{\text{VOilHydropro}}$ = Variable operating cost for bio-oil hydroprocessing facility at location k , \$/metric ton
 c^{char} = Price of char, \$/metric ton
 c_w^{chem} = Price of chemical w , \$/metric ton
 c^{gasol} = Price of gasoline, \$/metric ton
 c^{diesel} = Price of diesel fuel, \$/metric ton
 c^{hydro} = Price of hydrogen, \$/metric ton
 c^{lignin} = Price of lignin, \$/metric ton
 $a_d^{\text{OilReform}}$ = Linear coefficient for bio-oil reforming capital cost in segment d
 $b_d^{\text{OilReform}}$ = Linear coefficient for bio-oil reforming capital cost in segment d
 $p_d^{\text{Min,OilReform}}$ = Minimum mass flow of bio-oil for reforming in segment d , metric ton/year
 $p_d^{\text{Max,OilReform}}$ = Maximum mass flow of bio-oil for reforming in segment d , metric ton/year
 a_d^{Chem} = Linear coefficient for chemicals production capital cost in segment d
 b_d^{Chem} = Linear coefficient for chemicals production capital cost in segment d
 $p_d^{\text{Min,Chem}}$ = Minimum mass flow of aqueous bio-oil for chemicals production in segment d , metric ton/year
 $p_d^{\text{Max,Chem}}$ = Maximum mass flow of aqueous bio-oil for chemicals production in segment d , metric ton/year
 $a_d^{\text{OilHydropro}}$ = Linear coefficient for bio-oil hydroprocessing capital cost in segment d

$b_d^{\text{OilHydropro}}$ = Linear coefficient for bio-oil hydroprocessing capital cost in segment d
 $p_d^{\text{Min,OilHydropro}}$ = Minimum mass flow of bio-oil for hydroprocessing in segment d , metric ton/year
 $p_d^{\text{Max,OilHydropro}}$ = Maximum mass flow of bio-oil for hydroprocessing in segment d , metric ton/year
 $a_d^{\text{InsoluHydropro}}$ = Linear coefficient for water-insoluble bio-oil hydroprocessing capital cost in segment d
 $b_d^{\text{InsoluHydropro}}$ = Linear coefficient for water-insoluble bio-oil hydroprocessing capital cost in segment d
 $p_d^{\text{Min,InsoluHydropro}}$ = Minimum mass flow of water-insoluble bio-oil for hydroprocessing in segment d , metric ton/year
 $p_d^{\text{Max,InsoluHydropro}}$ = Maximum mass flow of water-insoluble bio-oil for hydroprocessing in segment d , metric ton/year
 $a_d^{\text{AquReform}}$ = Linear coefficient for aqueous phase bio-oil reforming capital cost in segment d
 $b_d^{\text{AquReform}}$ = Linear coefficient for aqueous phase bio-oil reforming capital cost in segment d
 $p_d^{\text{Min,AquReform}}$ = Minimum mass flow of aqueous phase bio-oil reforming in segment d , metric ton/year
 $p_d^{\text{Max,AquReform}}$ = Maximum mass flow of aqueous phase bio-oil reforming in segment d , metric ton/year
 int = Interest rate
 α = Biomass collection factor
 ε = Biomass loss factor
 β^{oil} = Bio-oil conversion rate in fast pyrolysis facility
 β^{char} = Biochar conversion rate in fast pyrolysis facility
 Num^{Pyro} = Maximum number of the fast pyrolysis facilities
 θ^{aqu} = Aqueous phase bio-oil weight percentage in bio-oil
 θ^{insol} = Water-insoluble phase bio-oil weight percentage in bio-oil
 $\theta^{\text{hydro},1}$ = Hydrogen yield from aqueous phase reforming
 $\theta^{\text{hydro},2}$ = Hydrogen yield from bio-oil reforming
 $\theta^{\text{gasol},1}$ = Gasoline yield from water-insoluble phase hydroprocessing
 $\theta^{\text{gasol},2}$ = Gasoline yield from bio-oil hydroprocessing
 $\theta^{\text{diesel},1}$ = Diesel fuel yield from water-insoluble phase hydroprocessing
 $\theta^{\text{diesel},2}$ = Diesel fuel yield from bio-oil hydroprocessing
 θ^{chem} = Chemical w yield from aqueous phase reforming
 $\delta^{\text{hydro},1}$ = Hydrogen requirement factor for chemicals production from aqueous phase bio-oil
 $\delta^{\text{hydro},2}$ = Hydrogen requirement factor for water-insoluble phase bio-oil hydroprocessing
 $\delta^{\text{hydro},3}$ = Hydrogen requirement factor for bio-oil hydroprocessing
 t = Project year for annualized capital cost

REFERENCES

- (1) Sissine, F. *Energy Independence and Security Act of 2007: a Summary of Major Provisions*; Library Of Congress Congressional Research Service: Washington, DC, 2007.
- (2) Coyle, W. T. *Next-Generation Biofuels Near-Term Challenges and Implications for Agriculture*; Report No. BIO-01-01; United States Department of Agriculture Economic Research Service: Washington, DC, 2010.
- (3) Brown, R. C. *Thermochemical Processing of Biomass: Conversion into Fuels*; John Wiley & Sons: New York, 2011; Vol. 12.
- (4) Bridgwater, A. V. Review of fast pyrolysis of biomass and product upgrading. *Biomass Bioenergy* **2012**, 38 (0), 68–94.
- (5) Bridgwater, A. V.; Peacocke, G. V. C. Fast pyrolysis processes for biomass. *Renewable Sustainable Energy Rev.* **2000**, 4 (1), 1–73.
- (6) Wang, D.; Czernik, S.; Montané, D.; Mann, M.; Chornet, E. Biomass to Hydrogen via Fast Pyrolysis and Catalytic Steam

Reforming of the Pyrolysis Oil or Its Fractions. *Ind. Eng. Chem. Res.* **1997**, *36* (5), 1507–1518.

(7) Zhu, X.-f.; Lu, Q. Selective Fast Pyrolysis of Biomass to Produce Fuels and Chemicals. In *Advanced Biofuels and Bioproducts*; Lee, J. W., Ed.; Springer: New York, 2013; pp 129–146.

(8) Karanjkar, P. U.; Coolman, R. J.; Huber, G. W.; Blatnik, M. T.; Almalkie, S.; de Bruyn Kops, S. M.; Mountziaris, T. J.; Conner, W. C. Production of aromatics by catalytic fast pyrolysis of cellulose in a bubbling fluidized bed reactor. *AIChE J.* **2014**, *60* (4), 1320–1335.

(9) Cheng, Y.-T.; Wang, Z.; Gilbert, C. J.; Fan, W.; Huber, G. W. Production of p-xylene from biomass by catalytic fast pyrolysis using ZSM-5 catalysts with reduced pore openings. *Angew. Chem., Int. Ed.* **2012**, *51* (44), 11097–11100.

(10) Chiaramonti, D.; Oasmaa, A.; Solantausta, Y. Power generation using fast pyrolysis liquids from biomass. *Renewable Sustainable Energy Rev.* **2007**, *11* (6), 1056–1086.

(11) Zhang, Y.; Brown, T. R.; Hu, G.; Brown, R. C. Comparative techno-economic analysis of biohydrogen production via bio-oil gasification and bio-oil reforming. *Biomass Bioenergy* **2013**, *51* (0), 99–108.

(12) Wright, M. M.; Daugaard, D. E.; Satrio, J. A.; Brown, R. C. Techno-economic analysis of biomass fast pyrolysis to transportation fuels. *Fuel* **2010**, *89* (Supplement1), S2–S10.

(13) Jones, S. B.; Valkenburg, C.; Walton, C. W.; Elliott, D. C.; Holladay, J. E.; Stevens, D. J.; Kinchin, C.; Czernik, S. *Production of Gasoline and Diesel from Biomass via Fast Pyrolysis, Hydrotreating and Hydrocracking: A Design Case*; Report No. PNNL-18284; Pacific Northwest National Laboratory: Richland, WA, 2009.

(14) Zhang, Y.; Brown, T. R.; Hu, G.; Brown, R. C. Techno-economic analysis of two bio-oil upgrading pathways. *Chem. Eng. J.* **2013**, *225* (0), 895–904.

(15) Zhang, Y.; Brown, T. R.; Hu, G.; Brown, R. C. Techno-economic analysis of monosaccharide production via fast pyrolysis of lignocellulose. *Bioresour. Technol.* **2013**, *127* (0), 358–365.

(16) Hsu, D. D. Life cycle assessment of gasoline and diesel produced via fast pyrolysis and hydroprocessing. *Biomass Bioenergy* **2012**, *45* (0), 41–47.

(17) Zhang, Y.; Hu, G.; Brown, R. C. Life cycle assessment of the production of hydrogen and transportation fuels from corn stover via fast pyrolysis. *Environ. Res. Lett.* **2013**, *8* (2), 025001.

(18) Zhang, Y.; Hu, G.; Brown, R. Life cycle assessment of commodity chemical production from forest residue via fast pyrolysis. *Int. J. Life Cycle Assess.* **2014**, *19* (7), 1371–1381.

(19) Kim, J.; Realff, M. J.; Lee, J. H.; Whittaker, C.; Furtner, L. Design of biomass processing network for biofuel production using an MILP model. *Biomass Bioenergy* **2011**, *35* (2), 853–871.

(20) Li, Y.; Hu, G. A sequential fast pyrolysis facility location-allocation model. In *Advances in Production Management Systems. Sustainable Production and Service Supply Chains*; Prabhu, V., Taisch, M., Kiritsis, D., Eds.; Springer: Berlin/Heidelberg, 2013; Vol. 414, pp 409–415.

(21) You, F.; Wang, B. Life cycle optimization of biomass-to-liquid supply chains with distributed–centralized processing networks. *Ind. Eng. Chem. Res.* **2011**, *50* (17), 10102–10127.

(22) Gebreslassie, B. H.; Yao, Y.; You, F. Design under uncertainty of hydrocarbon biorefinery supply chains: Multiobjective stochastic programming models, decomposition algorithm, and a comparison between CVaR and downside risk. *AIChE J.* **2012**, *58* (7), 2155–2179.

(23) Tong, K.; Gong, J.; Yue, D.; You, F. Stochastic programming approach to optimal design and operations of integrated hydrocarbon biofuel and petroleum supply chains. *ACS Sustainable Chem. Eng.* **2013**, *2* (1), 49–61.

(24) Kim, J.; Sen, S. M.; Maravelias, C. T. An optimization-based assessment framework for biomass-to-fuel conversion strategies. *Energy Environ. Sci.* **2013**, *6* (4), 1093–1104.

(25) Panichelli, L.; Gnansounou, E. GIS-based approach for defining bioenergy facilities location: A case study in Northern Spain based on marginal delivery costs and resources competition between facilities. *Biomass Bioenergy* **2008**, *32* (4), 289–300.

(26) Zhang, F.; Johnson, D. M.; Sutherland, J. W. A GIS-based method for identifying the optimal location for a facility to convert forest biomass to biofuel. *Biomass Bioenergy* **2011**, *35* (9), 3951–3961.

(27) Lin, T.; Rodríguez, L. F.; Shastri, Y. N.; Hansen, A. C.; Ting, K. C. GIS-enabled biomass-ethanol supply chain optimization: Model development and Miscanthus application. *Biofuels, Bioprod. Biorefin.* **2013**, *7* (3), 314–333.

(28) Zhang, Y.; Hu, G.; Brown, R. C. Integrated supply chain design for commodity chemicals production via woody biomass fast pyrolysis and upgrading. *Bioresour. Technol.* **2014**, *157* (0), 28–36.

(29) Sammons, N. E., Jr.; Yuan, W.; Eden, M. R.; Aksoy, B.; Cullinan, H. T. Optimal biorefinery product allocation by combining process and economic modeling. *Chem. Eng. Res. Des.* **2008**, *86* (7), 800–808.

(30) Murillo-Alvarado, P. E.; Ponce-Ortega, J. M.; Serna-González, M.; Castro-Montoya, A. J.; El-Halwagi, M. M. Optimization of pathways for biorefineries involving the selection of feedstocks, products, and processing steps. *Ind. Eng. Chem. Res.* **2013**, *52* (14), 5177–5190.

(31) Mansoornejad, B.; Chambost, V.; Stuart, P. Integrating product portfolio design and supply chain design for the forest biorefinery. *Comput. Chem. Eng.* **2010**, *34* (9), 1497–1506.

(32) Chen, Y.; Adams, T. A.; Barton, P. I. Optimal design and operation of static energy polygeneration systems. *Ind. Eng. Chem. Res.* **2010**, *50* (9), 5099–5113.

(33) Chen, Y.; Adams, T. A.; Barton, P. I. Optimal design and operation of flexible energy polygeneration systems. *Ind. Eng. Chem. Res.* **2011**, *50* (8), 4553–4566.

(34) Wright, M. M.; Román-Leshkov, Y.; Green, W. H. Investigating the techno-economic trade-offs of hydrogen source using a response surface model of drop-in biofuel production via bio-oil upgrading. *Biofuels, Bioprod. Biorefin.* **2012**, *6* (5), 503–520.

(35) Wright, M.; Brown, R. C. Establishing the optimal sizes of different kinds of biorefineries. *Biofuels, Bioprod. Biorefin.* **2007**, *1* (3), 191–200.

(36) Wright, M. M.; Satrio, J. A.; Brown, R. C.; Daugaard, D. E.; Hsu, D. D. *Techno-Economic Analysis of Biomass Fast Pyrolysis to Transportation Fuels*; Technical Report No. NREL/TP-6A20-46586; National Renewable Energy Laboratory: Golden, CO, 2010.

(37) MATLAB version 7.10.0. The MathWorks Inc.: Natick, MA, 2010.

(38) Grossmann, I. E.; Viswanathan, J.; Vecchiotti, A.; Raman, R.; Kalvelagen, E. *GAMS/DICOPT: A Discrete Continuous Optimization Package*; GAMS Development Corporation: Washington, DC, 2002.

(39) NREL Forest and Primary Mill Residues. http://www.nrel.gov/gis/data_biomass.html (accessed in 2013).

(40) Leinonen, A. *Harvesting Technology of Forest Residues for Fuel in the USA and Finland*; Research Notes 2229; VTT: Espoo, Finland, 2004.

(41) Bureau of Transportation Statistics. *Average Freight Revenue per Ton-mile*; Table 3-21; Bureau of Transportation Statistics: Washington, DC, 2012.

(42) Wright, M. M.; Brown, R. C.; Boateng, A. A. Distributed processing of biomass to bio-oil for subsequent production of Fischer–Tropsch liquids. *Biofuels, Bioprod. Biorefin.* **2008**, *2* (3), 229–238.

(43) Brown, T. R.; Zhang, Y.; Hu, G.; Brown, R. C. Techno-economic analysis of biobased chemicals production via integrated catalytic processing. *Biofuels, Bioprod. Biorefin.* **2012**, *6* (1), 73–87.

(44) Minnesota Gas Prices <http://www.minnesotagasprices.com/> (accessed in 2013).

(45) Jack, M. W. Scaling laws and technology development strategies for biorefineries and bioenergy plants. *Bioresour. Technol.* **2009**, *100* (24), 6324–6330.

(46) Wakeley, H.; Griffin, W.; Hendrickson, C.; Matthews, H. Alternative transportation fuels: Distribution infrastructure for hydrogen and ethanol in Iowa. *J. Infrastruct. Syst.* **2008**, *14* (3), 262–271.